

A review of solar radiation on vertically mounted solar surfaces and proper azimuth angles in six Iranian major cities

Kasra Mohammadi, Hossein Khorasanizadeh*

Faculty of Mechanical Engineering and the Energy Research Institute, University of Kashan, Kashan, Iran

ARTICLE INFO

Article history:

Received 26 July 2014

Received in revised form

3 February 2015

Accepted 8 March 2015

Available online 30 March 2015

Keywords:

Surface azimuth angle

Vertically mounted solar surfaces

Solar radiation

Solar energy gain

Iran

ABSTRACT

To meet a part of the buildings energy demands, the buildings' exterior walls are proper places for installation of vertically mounting solar surfaces (VMSS). In this study, using long-term horizontal global solar radiation data and the Klein and Theilacke radiation model, the solar radiation components arrived at VMSS have been assessed at different periods of the year and better surface azimuth angles have been suggested for six Iranian major cities of Isfahan, Karaj, Mashhad, Shiraz, Tabriz and Tehran. The results demonstrate that the beam and global solar radiation on non-azimuth VMSS (south walls) decline significantly in spring and summer compared to those of horizontal surface, though they are higher in most months of autumn and winter. The highest relative gains are in December, while the highest relative losses occur in June and they increase with increasing the latitude. In general, the total radiation on a vertical surface depends on its azimuth angle significantly and for each city its variation with azimuth angle is distinctive. Considering three practical azimuth angles of 0° , 45° and 90° , during the colder period (October–March) the buildings' south walls and during the warmer period (April–September) the east and west walls (i.e. azimuth angles of 90° and -90°) are suitable ones, respectively.

© 2015 Elsevier Ltd. All rights reserved.

Contents

1. Introduction	504
2. Literature survey	506
3. Data collection	507
4. Methodology	508
4.1. Modeling the solar radiation on a vertical surface at different azimuth angles	508
4.2. Computation procedures	509
5. Results and discussion	509
5.1. Solar radiation components on horizontal surface and clearness index	512
5.2. Solar radiation components on vertically mounted solar surfaces	512
5.3. Recognizing the better surface azimuth angles among practicable options	514
6. Conclusions	517
Acknowledgements	517
References	517

1. Introduction

In recent decades, the dramatic escalations in global energy demands along with environmental issues have brought some serious concerns regarding the future status of the world. Owing to the rapid growth in world population as well as the needs for a more comfortable life, the energy consumption is increasing enormously [1–3].

* Correspondence to: University of Kashan, Kashan 8731751167, Iran.

E-mail addresses: kasra278@yahoo.com (K. Mohammadi),

khorasan@kashanu.ac.ir (H. Khorasanizadeh).

Nomenclature

D	ratio of monthly mean beam radiation on a tilted surface to that on a horizontal surface
G	empirical functions obtained using Eq. (18)
G_{sc}	solar constant (equal to 1367 W/m ²)
\bar{H}	monthly mean daily global radiation on a horizontal surface (MJ/m ²)
\bar{H}_b	monthly mean daily beam radiation on a horizontal surface (MJ/m ²)
\bar{H}_{bv}	monthly mean daily beam radiation on a vertical surface (MJ/m ²)
\bar{H}_d	monthly mean daily diffuse radiation on a horizontal surface (MJ/m ²)
\bar{H}_{dv}	monthly mean daily diffuse radiation on a vertical surface (MJ/m ²)
\bar{H}_o	monthly mean daily extraterrestrial on a horizontal surface (MJ/m ²)
\bar{H}_v	monthly mean daily global radiation on a vertical surface (MJ/m ²)

\bar{K}_T	clearness index
n_{day}	day number
\bar{R}	ratio of monthly mean total radiation on a tilted surface to that on a horizontal surface

Greek letters

α_s	solar altitude angle (°)
β	surface slope angle (°)
γ	surface azimuth angle (°)
δ	solar declination angle (°)
ρ_g	ground reflectivity coefficient
φ	latitude of the location (°)
ω_s	sunset hour angle for a horizontal surface (°)
ω_{ss}	sunset hour angle for beam radiation on a tilted surface (°)
ω_{sr}	sunrise hour angle for beam radiation on a tilted surface (°)

Generating energy in large scales by exploitation of fossil fuels has led to perilous influence on the environment such as global warming, climate change, air pollution and water contamination [4–6]. In view of the obligations imposed by some international agreements on environmental policy, such as the Kyoto protocol to diminish the aforementioned hazardous threats, harnessing the renewable energies including solar, wind, geothermal, tidal and biomass have been adapted by governments as the most efficient solutions [7]. The development of renewable energy technologies are expanding greatly. By the end of 2013 the total renewable energy capacity across the world, not including hydro, reached to 560 GW from 480 GW at the end of 2012 [8]. Among different kind of renewables, solar energy is considered to be the most promising and appealing renewable source to meet the energy demands in the future [9]. About the significance of solar energy it is worthwhile to state that in case of converting only 0.1% of the solar energy arrived at the earth surface to electricity with the efficiency of 10%, the output power would be 3000 GW, which is four times higher than the current global consumption [10,11].

Several solar energy technologies have been invented so far. Among all, the flat plate solar collectors and photovoltaic panels are being increasingly utilized for heat and electricity generations. Generally, among several parameters that affect the performance of a flat plate solar surface its tilt and azimuth angles stand out above all. The notability of these angles for a surface is owing to the fact that their variation would change the amount of solar radiation arriving at it.

Technically, the most efficient method to collect more solar energy is to utilize tracking systems. A solar tracker system is a mechanical tool designed to follow the direction of the sun in the sky to gain maximum possible energy. Nonetheless, in spite of achieving more energy via utilization of solar tracking systems, in some cases the required costs exceed the extra energy achieved. This makes the system to become economically unfeasible and inapplicable. Therefore, to receive more energy it is often viable to adjust the solar surface at optimal tilt and azimuth angles for specified periods such as day, month or season.

Basically, the knowledge of global solar radiation received by a tilted surface as well its optimal tilt angle are of particular importance to design, optimize and monitor the performance of solar energy conversion systems [12–14]. Likewise, the information about different components of solar radiation, either in terms of daily or

monthly mean daily values, arriving at a surface with the optimum surface azimuth is also of indispensable significance for solar energy systems design and simulation procedures. The amount of radiation arrived at an oriented surface in different specific periods of the year is contingent upon several elements including the local solar radiation characteristics and climatic conditions, latitude and the specific period of time that the system is utilized.

There are three possible major options in order to mount the solar surfaces for the sake of solar energy harnessing: (1) on the ground, (2) on the roof of buildings and (3) on the vertical walls of buildings. In the case of lacking enough roof space on a building, mounting the photovoltaic panels and thermal collectors on the exterior vertical walls of buildings is an option. Moreover, the low level of requisite costs for construction, installation and structural materials of wall-mounted solar systems is a merit. Fig. 1 shows the PV panels mounted on the exterior walls of a building in San Diego, which is part of the largest project of this kind in the USA.

Iran is one of the countries located in solar belt of the world and the solar energy is abundantly available in most parts of the country, which provides the possibility of taking the advantage of harnessing solar energy via various technologies. Nevertheless, only a limited number of solar energy projects have been established in Iran. Also, the number of investigations related to solar energy is still limited.



Fig. 1. Solar panels mounted vertically on the walls of a building in San Diego, USA [15].

The primary reason and barrier is the abundant reserves of oil and gas in Iran, so that the nominal cost of energy generation using fossil fuels based sources has always been low. The first PV solar site in Iran was established in Doorbid region of Yazd province in 1993 with capacity of 5 kW DC. Later in 1998 the second site was developed in Hosseinian and Moalleman villages located in Semnan province with the total capacity of 27 kW AC. In 2012, the capacity of these sites has been enhanced to 10 kW DC and 92 kW AC, respectively. The total amount of electricity generation from solar power plants, with some fluctuations from one year to another, has been reported around 67 MW in 2012 [16]. At current time, 11 solar energy projects are being utilized in different parts of Iran to meet a part of energy demands of the country, particularly for some rural areas with no easy access to electricity [16]. Generally, utilization of solar tracking systems for improving the efficiency of solar energy harnessing specially in big projects is rare. Due to the increment of energy demands as well as remarkable increase in the level of greenhouse gases especially in the major cities of Iran, further attention and investigation is required to develop and harness the solar energy effectively. On this account, in this research work the amounts of solar radiation components on vertically mounted solar surfaces at different azimuth angles for six major Iranian cities are assessed and afterwards the appropriate practical azimuth angles are introduced.

The organization of the rest of the paper is as follows: Section 2 presents the literature survey regarding the tilt and surface azimuth angles optimization and the outlines of this study. In Section 3 the data collection is presented. Section 4 offers the utilized methodology and mathematical models. The results and discussion are brought forward in Section 5. Finally, the conclusions are presented in Section 6.

2. Literature survey

Optimal tilt and surface azimuth angles have a notable influence on the performance of flat plate solar surfaces. In this regard, several models have been proposed by different researchers to calculate the total solar radiation on the inclined surfaces by utilizing the available data for horizontal surfaces [17–33]. Nonetheless, due to climate and location dependency of the tilt and azimuth angles each place has its own values. Several studies have dealt with optimizing the tilt and azimuth angles of flat plate solar collectors and PV panels using various mathematical models for many locations around the world, however, only some selected ones are reviewed in brief in the following, purposely.

Tsalides and Thanailakis [34] presented a general model to determine the optimal tilt angle of solar PV arrays, taking into account the latitude, climatic and radiation conditions as well as the orientation of the PV. They obtained the optimum tilt angles for both south-facing and off-south facing PVs for several locations in Greece. Morcos [35] determined the optimum tilt and azimuth angles of solar collectors for installation in Assiut, Egypt. The results indicated that for the surfaces with no azimuth angle changing the tilt angle eight times per year is required to attain a total solar radiation around its maximum value. Also, by changing the surface azimuth angle 12 times and the tilt angle six times during a year, the solar radiation arriving at the surface would become the maximum. Hussein et al. [36] examined the influence of the tilt and azimuth angles on the performance of PV modules in Cairo, Egypt. Their results illustrated that the highest yearly performance is obtained by adjusting the modules toward the south with a fixed tilt between 20° and 30°. Furthermore, by adjusting a PV module toward the west it receives higher annual solar energy compared with that of the one toward east. Tang and Wu [37] conducted an investigation to estimate the monthly optimum tilt angle of the south-facing collectors in China. They presented a contour map of the optimum tilt angle based upon the solar data of 152 locations. By

analyzing the effect of surface azimuth angle on optimal tilt angle they concluded that with increment of the azimuth angle the optimum tilt angle would be declined. Gunerhan and Hepbasli [38] performed a study to find the optimal tilt and azimuth angles of solar collectors for building applications in city of Izmir, Turkey. They illustrated that the best orientation for solar collectors is facing them toward the south and to attain higher level of solar radiation the tilt angle of solar collector should be adjusted each month. Gopinathan et al. [39] carried out an investigation on estimation of monthly average daily global solar radiation at various slopes and orientations for three locations in the Southern African, utilizing the anisotropic model proposed by Hay. They obtained the optimal tilt and azimuth angles for the winter and summer periods as well as the whole year. According to their results, at any slope the maximum solar radiation is achieved at azimuth of 180° (facing equator). Also, the yearly optimum tilt angle was reported equal to the latitude and latitude minus 10°, respectively, for low and high azimuth angles. Rowlands et al. [40] conducted a study to determine the yearly tilt and azimuth angles of a PV panel for receiving more solar radiation at two different locations of Canada. The achieved results revealed that the optimum tilt angle is a little lower than the latitude and the optimal azimuth direction is toward the south with only a minor deviation. Sunderan et al. [41] showed that the optimum tilt angle and orientation enhance the power generation of Standalone Photovoltaic Electricity Generation Systems (SPVEGS) in Ipoh, Malaysia. They found that the optimum orientation of a PV module is due north from April to August and is due south for the remaining months. Sun et al. [42] performed an investigation to calculate the optimum tilt angle for the shading-type Building Integrated Photovoltaic (BIPV) claddings at different orientations in Hong Kong. Their results demonstrated that the highest electricity generation per unit area is obtained if the PV modules are installed on south facades at the tilt angle of 10°. Talebizadeh et al. [43] utilized the Genetic algorithm to predict the optimum tilt and azimuth angles for a location in Iran in terms of hourly, daily, monthly, seasonally and yearly analysis. They also studied the effect of different solar radiation components on the optimal tilt angle as well as the amount of energy gain. Their results specified that installing the solar collector at the hourly optimum tilt and azimuth angles leads to notable enhancement of the solar radiation received compared with that of the daily optimum adjustment strategy. Jafarkazemi and Saadabadi [44] focused on determining the effect of orientation on the optimum tilt angle of solar collectors and solar panels in Abu Dhabi, UAE. Their results showed that the annual optimum tilt angle is close to latitude of Abu Dhabi and the optimal orientation is towards south direction. Also, to receive more radiation they suggested adjusting the tilt angle at least twice a year. They also performed a short study on the vertical solar surfaces and determined the annual optimum azimuth angle.

In some other investigations different types of solar tracking systems have been evaluated and their performances compared with those of the optimally tilted and oriented ones. Kacira et al. [45] utilized a mathematical model to estimate the optimum tilt and orientation angles for a PV panel installed in Sanliurfa, Turkey. Their results illustrated that by mounting the PV panel at the monthly optimum tilt angle 12 times throughout the year, 1.1% and 3.9% more energy is gained compared with those of adjusted seasonally at optimum tilt and the one adjusted annually with a tilt angle equal to latitude, respectively. Furthermore, by using a two-axis solar tracking system 29.3% more solar radiation is gained compared with that of a fixed south facing panel. Ghosh et al. [46] utilized three different mathematical models to determine the monthly and seasonal optimum tilt angles of solar collectors in Dhaka, the capital of Bangladesh. They also investigated the possibility of gaining more solar radiation by switching the azimuth angle between −45° and +45° as well as utilizing tracking systems. The results showed that the annual solar radiation gains utilizing different strategies including

the monthly and seasonal optimum tilt adjustments, optimum azimuth angle adjustment in the range of $\pm 45^\circ$ as well as utilizing the single and double axis tracking systems compared to that of a surface with a fixed slope equal to the latitude are 8%, 4%, 14%, 22% and 25%, respectively. Lave and Kleissl [47] calculated the optimal tilt and azimuth angles of solar panels in the continental United States. They compared the annual global radiation incident on a panel at different optimum orientations with that of a flat horizontal panel as well as a 2-axis tracking panel. They found that with increasing latitude, the irradiation at optimum fixed tilted panel increases between 10% and 25%. Also, irradiation incident on a 2-axis tracking panel is between 25% and 45% higher than irradiation on the panel at optimum fixed orientation. Lubitz [48] investigated the influence of tilt angle adjustment on solar radiation received by fixed and tracking solar surfaces at 217 stations across the USA. The optimum tilt angles for a fixed south-facing surface were between the latitude and 14° less than the latitude. For an azimuth tracking surface the optimum tilt was around 19° closer to vertical than that of a fixed surface at the same station. His results also demonstrated that utilizing the azimuth adjustment and two axis tracking surfaces improve the annual incident solar irradiation by an average of 29% and 34%, respectively, compared to a fixed south-facing surface at optimum tilt angle. Maatallah et al. [49] studied the influence of the azimuth and tilt angles on the output power of a PV panel for city of Monastir, Tunisia and also compared the output power generated by a single and dual-axis tracking system with a fixed panel. To enhance and optimize the system they suggested changing the azimuth angle from the south direction at early morning or late afternoon by using a dual-axis tracking system. This strategy resulted in gaining up to 30% and 44% more energy in the winter and summer days, respectively.

In recent years, two review papers have been published in the realms of optimizing the tilt and azimuth angles as well as utilizing the tracking systems to receive more radiation. Yadav and Chandel [50] provided an overview on optimization of the solar surface tilt and azimuth angles using various methods and mathematical models. Their review showed that the optimal angles of a solar surface should be determined individually for every specific location. Also, Mousazadeh et al. [51] reviewed and discussed different types of sun-tracking solar systems. They indicated that among all, the polar-axis and azimuth/elevation types are the most effective and well-known sun-tracking devices.

Review of the literature reveals that the conducted researches in this area have focused on: (1) Calculating the amount of solar radiation arrived at solar surfaces with different tilt and azimuth angles and determining the optimum tilt and azimuth angles. (2) Evaluating the solar radiation received by different types of solar tracking surfaces and providing comparisons with the optimally tilted and oriented surfaces. However, no study has been devoted specifically to assess the solar radiation on the fixed wall-mounted solar surfaces. This study aims at calculating the solar radiation components on vertically mounted solar surfaces at different azimuth angles and introducing better azimuth angles in the warm and cold periods of the year in six major cities of Iran. The long-term daily horizontal global solar radiation data, taken from Iranian Meteorological Organization (IMO), have been used for the cities of Isfahan, Karaj, Mashhad, Shiraz, Tabriz and Tehran. These cities have been nominated in view of the fact that they are developing faster and for them solar energy utilization is being of paramount importance.

3. Data collection

In this study, long-term daily global solar radiation data on a horizontal surface provided by the Iranian meteorological organization (IMO) for the six Iranian major cities of Isfahan, Karaj, Mashhad, Shiraz,

Tabriz and Tehran have been utilized. These cities, as shown in Fig. 2, are placed in different geographical locations of Iran and have different climatic conditions. As highlighted on the map, every city is the center of one particular Iranian province. The geographical location, elevation from the sea level as well as the measurement time period of data for the nominated cities are presented in Table 1. In the solar data provided by IMO there were differences in the number and distributions of the measurement years. Also, the data collections for these cities contained some missing and incorrect values possibly due to instruments' malfunction. Thus, prior to any attempt for data analysis, the quality of solar data was enhanced using the following simple procedure:

- (1) To identify the incorrect global solar radiation values, the concept of daily clearness index (K_T) was used as a benchmark. All daily values which resulted in a daily clearness index out of range ($0.015 < K_T < 1$) were eliminated [52,53].
- (2) The data for a month containing more than 5 days missing or unreliable global solar radiation values were completely withdrawn. Additionally, for a month with less than 5 days missing or inaccurate values proper daily values were substituted by means of interpolation [52,53].

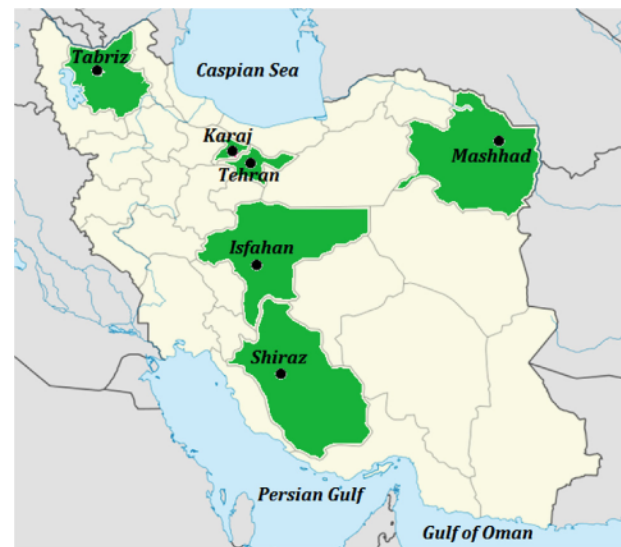


Fig. 2. Location of the six nominated cities on the map of Iran (the corresponding provinces are highlighted).

Table 1

The geographical location and the provided solar data utilized for the six nominated cities.

City (province)	Latitude (N)	Longitude (E)	Elevation (m)	Data period
Isfahan (Isfahan)	32°37'	51°40'	1550.4	1985–2005
Karaj (Alborz)	35°55'	50°54'	1312.5	1985–1996
Mashhad (Razavi Khorasan)	36°16'	59°38'	999.2	1980–1999
Shiraz (Fars)	29°32'	56°36'	1484.0	1982–2000
Tabriz (East Azerbaijan)	38°50'	46°17'	1361.0	1992–2005
Tehran (Tehran)	35°48'	51°29'	1549.1	1993–2005

After data cleaning process to achieve the monthly mean daily global radiation values, first, an average was obtained for each day of the year by using the measured daily global solar radiation values related to different years in the data series. Afterwards these averaged daily values were utilized to obtain the monthly mean daily values.

4. Methodology

In this section, the mathematical representation as well as the computational procedures employed to estimate the solar radiation arriving at vertically mounted solar surfaces at different surface azimuth angles are introduced and explained. Prior to any explication some related solar basics are reviewed briefly.

On average, the amount of extraterrestrial radiation incident on a plane perpendicular to the sun rays is defined as solar constant, G_{sc} , and is typically considered equal to 1367 W/m^2 . However, solar attenuation occurs as radiation passes through the atmosphere due to some atmospheric phenomenon such as aerosol extinction, cloud extinction, permanent gas absorption, ozone absorption, Rayleigh scattering and water vapor absorption. The extraterrestrial solar radiation on a horizontal surface, H_o , for each day of the year is calculated via [54,55]:

$$H_o = \frac{24 \times 3600}{\pi} G_{sc} \left(1 + 0.033 \cos \frac{360 n_{day}}{365} \right) \times \left(\cos \varphi \cos \delta \sin \omega_s + \frac{\pi \omega_s}{180} \sin \varphi \sin \delta \right) \quad (1)$$

where φ is the latitude of the location and n_{day} is the day of the year numbered from January 1st. The declination, δ , is the angular position of the sun at solar noon with respect to the equator plane, which take values in the range of $-23.45^\circ \leq \delta \leq 23.45^\circ$. The angular displacement of the sun with respect to the local meridian, owing to rotation of the earth on its axis at rate of $15^\circ/\text{h}$, is expressed by concept of the hour angle, ω . This angle is zero at solar noon, negative in the morning and positive in the afternoon. ω_s is the sunset hour angle used to derive the time of sunset for every latitude and solar declination. δ and ω_s are obtained, respectively, via [54,55]:

$$\delta = 23.45 \sin \left(\frac{(n_{day} + 284) 360}{365} \right) \quad (2)$$

$$\omega_s = \cos^{-1}(-\tan \varphi \tan \delta) \quad (3)$$

It is worthwhile to mention that for the case of monthly mean daily analysis the recommended average day of each month [54] is used for calculation purposes.

The position of the sun in the sky can be described by solar altitude angles, α_s , which is the angle between the line directed to the sun and a horizontal plane. The tilt angle, β , specifies how far a surface is inclined from the horizontal plane and it usually varies between 0° and $+90^\circ$. For a horizontal surface $\beta=0^\circ$ and for a vertical surface $\beta=90^\circ$. The surface azimuth angle, γ , is the angle between the horizontal extension of the normal to the surface and the north–south coordinate. Fig. 3 schematically illustrates the solar altitude angle, α_s , the surface tilt angle, β , and its azimuth angle, γ . The azimuth angle for a vertical surface facing towards east is negative and towards west is positive. For the surface shown in Fig. 3 the azimuth angle is negative. The azimuth angle of zero is for southward surfaces, -90° for eastward surfaces, $+90^\circ$ for westward surfaces and 180° for northward surfaces.

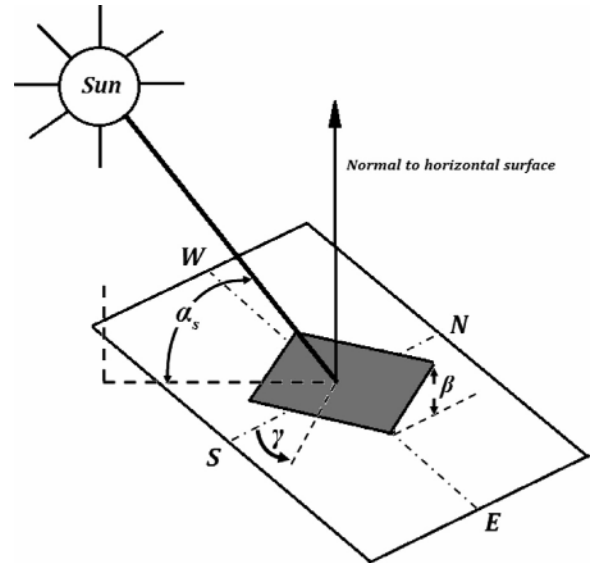


Fig. 3. The altitude angle of sun (α_s), the surface tilt (β) and azimuth (γ) angles.

4.1. Modeling the solar radiation on a vertical surface at different azimuth angles

For estimating the total monthly mean daily solar radiation reached on a vertically mounted solar surface at different surface azimuth angles as well as determining the better surface azimuth angle the KT method developed by Klein and Theilacker [33] has been utilized. Duffie and Beckman [54] noted that the suggested mathematical models by Klein and Theilacker [33] are valid for all azimuth angles and geographical locations. In this method the diffuse and ground-reflected radiations are both isotropic. The monthly mean daily total solar radiation incident on a tilted surface, based upon the KT model, is defined as:

$$\bar{H}_T = \bar{H} \times R \quad (4)$$

\bar{H} is the monthly mean daily global radiation on a horizontal surface. \bar{R} , the ratio of monthly mean daily global solar radiation on an inclined surface to that on a horizontal surface, is the combination of three terms of beam, diffuse and ground reflected and is expressed as [33]:

$$\bar{R} = D + \frac{\bar{H}_d}{\bar{H}} \left(\frac{1 + \cos \beta}{2} \right) + \rho_g \left(\frac{1 - \cos \beta}{2} \right) \quad (5)$$

For the case of a vertical surface, $\beta=90^\circ$ and Eq. (5) is expressed in the simple form of:

$$\bar{R} = D + 0.5 \frac{\bar{H}_d}{\bar{H}} + 0.5 \rho_g \quad (6)$$

D is the ratio of the monthly mean daily beam radiation on a tilted surface to the monthly mean daily global radiation on a horizontal surface. \bar{H}_d is the monthly mean daily diffuse radiation on a horizontal surface and ρ_g is the ground reflectivity coefficient. D is given by [33]:

$$D = \begin{cases} \max(0, G(\omega_{ss}, \omega_{sr})) & \text{if } \omega_{ss} \geq \omega_{sr} \\ \max(0, [G(\omega_{ss}, -\omega_s) + G(\omega_s, \omega_{sr})]) & \text{if } \omega_{ss} \leq \omega_{sr} \end{cases} \quad (7)$$

ω_{ss} and ω_{sr} are the sunset and sunrise hour angles for beam radiation on a tilted surface, respectively. Clearly, two terms are appeared in the second part of Eq. (7) as for some orientations the sun can rise and set on the surface twice throughout a day [54]. The signs of ω_{ss} and ω_{sr} depend upon the surface orientation and would change

as described by [33]:

$$|\omega_{sr}| = \min \left[\omega_s, \cos^{-1} \left(\frac{AB + C\sqrt{A^2 - B^2 + C^2}}{A^2 + C^2} \right) \right] \quad (8)$$

$$\omega_{sr} = \begin{cases} -|\omega_{sr}| & \text{if } (A > 0 \ \& \ B > 0) \text{ or } A \geq B \\ +|\omega_{sr}| & \text{if otherwise} \end{cases} \quad (9)$$

$$|\omega_{ss}| = \min \left[\omega_s, \cos^{-1} \left(\frac{AB - C\sqrt{A^2 - B^2 + C^2}}{A^2 + C^2} \right) \right] \quad (10)$$

$$\omega_{ss} = \begin{cases} -|\omega_{ss}| & \text{if } (A > 0 \ \& \ B > 0) \text{ or } A \geq B \\ +|\omega_{ss}| & \text{if otherwise} \end{cases} \quad (11)$$

where A , B and C are functions of solar geometry and position of the solar surface defined by:

$$A = \cos \beta + \tan \varphi \cos \gamma \sin \beta \quad (12)$$

$$B = \cos \omega_s \cos \beta + \tan \delta \cos \gamma \sin \beta \quad (13)$$

$$C = (\sin \beta \sin \gamma / \cos \varphi) \quad (14)$$

For a vertically mounted surface A , B and C are simplified as

$$A = \tan \varphi \cos \gamma \quad (15)$$

$$B = \tan \delta \cos \gamma \quad (16)$$

$$C = (\sin \gamma / \cos \varphi) \quad (17)$$

The three empirical functions of G , appeared in Eq. (7), are defined as [33]:

$$G(\omega_1, \omega_2) = \frac{1}{2d} \left[\frac{\pi}{180} \left(\frac{bA}{2} - a'b \right) (\omega_1 - \omega_2) + ((a'A - bB) \times (\sin \omega_1 - \sin \omega_2)) - a'C (\cos \omega_1 - \cos \omega_2) \right] - \left(\frac{bA}{2} \right) (\sin \omega_1 \cos \omega_1 - \sin \omega_2 \cos \omega_2) + \left(\frac{bC}{2} \right) (\sin^2 \omega_1 - \sin^2 \omega_2) \quad (18)$$

ω_1 and ω_2 correspond with ω_{ss} , ω_{sr} and ω_s , which are presented in Eqs. (7)–(11). The parameters a , a' , b and d are obtained as:

$$a = 0.4090 + 0.5016 \sin(\omega_s - 60) \quad (19)$$

$$a' = a - \frac{\bar{H}_d}{\bar{H}} \quad (20)$$

$$b = 0.6609 - 0.4767 \sin(\omega_s - 60) \quad (21)$$

$$d = \sin \omega_s - (\pi \omega_s / 180) \cos \omega_s \quad (22)$$

Since only the global solar radiation on a horizontal surface are accessible for the six Iranian major cities, the monthly mean daily diffuse solar radiation on horizontal surface should be estimated. For this aim, the global solar radiation data were used to estimate monthly mean daily horizontal diffuse solar radiation using the correlation suggested by Erbs et al. [56] as:

for $\omega_s \leq 81.4^\circ$ and $0.3 \leq \bar{K}_T \leq 0.8$

$$\frac{\bar{H}_d}{\bar{H}} = 1.391 - 3.560\bar{K}_T + 4.189\bar{K}_T^2 - 2.137\bar{K}_T^3 \quad (23 - a)$$

for $\omega_s \geq 81.4^\circ$ and $0.3 \leq \bar{K}_T \leq 0.8$

$$\frac{\bar{H}_d}{\bar{H}} = 1.311 - 3.022\bar{K}_T + 3.427\bar{K}_T^2 - 1.821\bar{K}_T^3 \quad (23 - b)$$

\bar{K}_T is the monthly mean daily clearness index defined as the ratio of monthly mean daily global solar radiation on a horizontal surface, \bar{H} , to the monthly mean daily extraterrestrial solar radiation on a horizontal surface, \bar{H}_o , expressed as

$$\bar{K}_T = \frac{\bar{H}}{\bar{H}_o} \quad (24)$$

4.2. Computation procedures

Generally, for a solar surface with positive azimuth angle (i.e. west direction) the solar radiation reached on the surface enhances in the afternoon and declines at morning, if compared with a non-azimuth surface. Whereas, the solar incidence to a surface with negative azimuth angle (i.e. east direction) increases in the morning and decreases in the afternoon. Nevertheless, for similar absolute deviation of a solar surface either toward east or west the solar radiation arriving on the surface during a day is equal. As a consequence, only the positive azimuth angles or in other words adjusting the surface towards west is considered for the analysis.

To calculate different solar radiation components on vertical surfaces and recognize the more appropriate azimuth angle a computer program was developed in MATLAB software. In the program, the calculated values of monthly mean daily global, beam and diffuse radiation on a horizontal surface have been utilized to estimate the corresponding values on a particular vertical surface with the tilt angle equal to 90° . To determine the influence of variation of azimuth angle, γ , on the amount of solar radiation received by the vertical surfaces the γ has to be changed from 0° to 90° with interval of 1° . Nonetheless, as the vertical solar surfaces are mounted on the existing building's walls it is not practical to consider all γ values. Owing to the characteristics of

sun in northern hemisphere, the North–South, North East–South West and North West–South East are the suitable and usual orientations of buildings in Iran. Therefore, to identify the better azimuth angles in a particular time period, only three different γ values of 0° , 45° and 90° are considered. As mentioned earlier, the results obtained for γ equal to 45° and 90° are identical to those of -45° and -90° , respectively. The γ which leads to attaining the maximum value of monthly mean daily total solar radiation on the vertical surface, \bar{H}_v , is chosen by the program as the better azimuth angle for that month or time period. Most of the earth surface in all of the nominated cities are bare grounds and covered by snow only in few days throughout the year, thus the ground reflectivity coefficient, ρ_g , is considered to be 0.2 in all of the calculations [54].

5. Results and discussion

This section offers the most important results attained in this research work. The results are reported and discussed in different sections. In the first part, different components of horizontal solar radiation as well as clearness index on monthly mean daily basis are presented. Next, the of solar radiation components received by vertically mounted solar surfaces at different azimuth angles as well as the global and beam solar radiation gain compared to those of horizontal surface are discussed. Afterwards the results related

Table 2

Monthly mean daily global, beam, diffuse and extraterrestrial solar radiations on horizontal surface as well as monthly mean daily clearness index in the six nominated cities.

Location	Months	\bar{H}	\bar{H}_b	\bar{H}_d	\bar{H}_o	\bar{K}_T
Isfahan	Jan	11.80	8.18	3.61	19.86	0.59
	Feb	15.59	10.73	4.86	24.74	0.63
	Mar	19.30	13.26	6.04	30.68	0.63
	Apr	21.59	14.16	7.43	36.39	0.59
	May	25.58	17.80	7.78	40.02	0.64
	Jun	27.80	20.15	7.65	41.36	0.67
	Jul	26.77	19.11	7.66	40.60	0.66
	Aug	24.95	17.86	7.09	37.69	0.66
	Sep	21.95	15.91	6.04	32.67	0.67
	Oct	17.37	12.37	5.00	26.43	0.66
	Nov	12.57	8.77	3.80	20.97	0.60
	Dec	10.71	7.30	3.41	18.46	0.58
Karaj	Jan	10.67	7.41	3.26	17.94	0.59
	Feb	12.27	7.85	4.42	23.03	0.53
	Mar	15.10	8.81	6.28	29.39	0.51
	Apr	19.69	12.18	7.51	35.73	0.55
	May	22.43	14.08	8.35	39.96	0.56
	Jun	23.56	14.89	8.66	41.59	0.57
	Jul	22.29	13.72	8.57	40.69	0.55
	Aug	21.27	13.52	7.75	37.28	0.57
	Sep	18.81	12.36	6.45	31.62	0.59
	Oct	14.40	9.26	5.13	24.85	0.58
	Nov	11.82	8.44	3.38	19.11	0.62
	Dec	10.36	7.47	2.89	16.51	0.63
Mashhad	Jan	8.72	5.28	3.44	17.56	0.50
	Feb	10.76	6.27	4.49	22.69	0.47
	Mar	12.33	6.07	6.26	29.13	0.42
	Apr	17.40	9.75	7.65	35.59	0.49
	May	21.11	12.62	8.49	39.93	0.53
	Jun	23.97	15.35	8.62	41.62	0.58
	Jul	24.68	16.47	8.21	40.70	0.61
	Aug	22.75	15.29	7.46	37.19	0.61
	Sep	19.83	13.67	6.16	31.41	0.63
	Oct	14.03	8.94	5.09	24.54	0.57
	Nov	10.24	6.67	3.56	18.74	0.55
	Dec	8.07	4.92	3.15	16.13	0.50
Shiraz	Jan	13.47	9.65	3.82	21.67	0.62
	Feb	16.23	10.98	5.25	26.32	0.62
	Mar	18.40	11.82	6.58	31.83	0.58
	Apr	22.18	14.69	7.49	36.92	0.60
	May	25.32	17.49	7.83	39.99	0.63
	Jun	27.36	19.69	7.66	41.05	0.67
	Jul	25.78	17.91	7.86	40.41	0.64
	Aug	24.20	16.80	7.40	37.99	0.64
	Sep	22.67	16.49	6.18	33.58	0.68
	Oct	19.13	14.12	5.02	27.87	0.69
	Nov	13.96	9.92	4.04	22.72	0.61
	Dec	12.90	9.39	3.51	20.31	0.64
Tabriz	Jan	6.64	3.41	3.23	16.13	0.41
	Feb	9.74	5.49	4.25	21.39	0.46
	Mar	13.15	7.09	6.06	28.12	0.47
	Apr	16.22	8.67	7.55	35.02	0.46
	May	20.01	11.47	8.53	39.80	0.50
	Jun	24.16	15.54	8.61	41.72	0.58
	Jul	22.99	14.50	8.49	40.69	0.56
	Aug	20.49	12.78	7.72	36.81	0.56
	Sep	17.79	11.49	6.30	30.56	0.58
	Oct	12.42	7.47	4.95	23.33	0.53
	Nov	8.53	5.12	3.41	17.35	0.49
	Dec	6.71	3.80	2.92	14.69	0.46
Tehran	Jan	7.92	4.33	3.59	17.98	0.44
	Feb	11.90	7.43	4.47	23.07	0.52
	Mar	15.33	9.06	6.27	29.42	0.52
	Apr	20.31	12.88	7.44	35.74	0.57
	May	24.45	16.44	8.01	39.96	0.61
	Jun	28.41	20.87	7.54	41.58	0.68
	Jul	25.67	17.68	7.99	40.69	0.63
	Aug	24.85	17.89	6.96	37.29	0.67
	Sep	21.02	15.09	5.93	31.65	0.66
	Oct	15.77	10.90	4.87	24.89	0.63
	Nov	10.01	6.31	3.70	19.15	0.52
	Dec	7.93	4.67	3.27	16.55	0.48

Table 3The monthly mean daily total, beam and diffuse solar radiations on the horizontal and non-azimuth vertical surfaces (MJ/m²) in the six nominated cities.

Location	Months	\bar{H}	\bar{H}_V	\bar{H}_b	\bar{H}_{bV}	\bar{H}_d	\bar{H}_{dV}
Isfahan	Jan	11.80	16.23	8.18	13.24	3.61	1.81
	Feb	15.59	16.38	10.73	12.39	4.86	2.43
	Mar	19.30	14.38	13.26	9.43	6.04	3.02
	Apr	21.59	10.84	14.16	4.97	7.43	3.71
	May	25.58	9.17	17.80	2.72	7.78	3.89
	Jun	27.80	8.32	20.15	1.72	7.65	3.82
	Jul	26.77	8.67	19.11	2.16	7.66	3.83
	Aug	24.95	10.61	17.86	4.57	7.09	3.54
	Sep	21.95	14.01	15.91	8.80	6.04	3.02
	Oct	17.37	16.60	12.37	12.36	5.00	2.50
	Nov	12.57	16.20	8.77	13.04	3.80	1.90
	Dec	10.71	15.70	7.30	12.93	3.41	1.70
Karaj	Jan	10.67	16.20	7.41	13.50	3.26	1.63
	Feb	12.27	13.51	7.85	10.07	4.42	2.21
	Mar	15.10	11.66	8.81	7.00	6.28	3.14
	Apr	19.69	10.75	12.18	5.02	7.51	3.76
	May	22.43	9.26	14.08	2.84	8.35	4.18
	Jun	23.56	8.58	14.89	1.89	8.66	4.33
	Jul	22.29	8.69	13.72	2.18	8.57	4.29
	Aug	21.27	10.22	13.52	4.22	7.75	3.87
	Sep	18.81	12.86	12.36	7.75	6.45	3.22
	Oct	14.40	14.28	9.26	10.27	5.13	2.57
	Nov	11.82	16.97	8.44	14.10	3.38	1.69
	Dec	10.36	17.50	7.47	15.03	2.89	1.44
Mashhad	Jan	8.72	12.34	5.28	9.75	3.44	1.72
	Feb	10.76	11.49	6.27	8.17	4.49	2.24
	Mar	12.33	9.26	6.07	4.90	6.26	3.13
	Apr	17.40	9.72	9.75	4.15	7.65	3.83
	May	21.11	9.02	12.62	2.67	8.49	4.24
	Jun	23.97	8.78	15.35	2.08	8.62	4.31
	Jul	24.68	9.31	16.47	2.74	8.21	4.10
	Aug	22.75	10.93	15.29	4.93	7.46	3.73
	Sep	19.83	13.84	13.67	8.77	6.16	3.08
	Oct	14.03	14.07	8.94	10.12	5.09	2.55
	Nov	10.24	14.14	6.67	11.34	3.56	1.78
	Dec	8.07	12.41	4.92	10.03	3.15	1.58
Shiraz	Jan	13.47	17.31	9.65	14.05	3.82	1.91
	Feb	16.23	15.67	10.98	11.42	5.25	2.62
	Mar	18.40	12.62	11.82	7.49	6.58	3.29
	Apr	22.18	10.29	14.69	4.33	7.49	3.74
	May	25.32	8.37	17.49	1.92	7.83	3.92
	Jun	27.36	7.54	19.69	0.98	7.66	3.83
	Jul	25.78	7.84	17.91	1.33	7.86	3.93
	Aug	24.20	9.59	16.80	3.47	7.40	3.70
	Sep	22.67	13.37	16.49	8.01	6.18	3.09
	Oct	19.13	17.16	14.12	12.74	5.02	2.51
	Nov	13.96	16.70	9.92	13.29	4.04	2.02
	Dec	12.90	18.00	9.39	14.95	3.51	1.76
Tabriz	Jan	6.64	9.12	3.41	6.84	3.23	1.61
	Feb	9.74	10.85	5.49	7.75	4.25	2.13
	Mar	13.15	10.58	7.09	6.24	6.06	3.03
	Apr	16.22	9.51	8.67	4.11	7.55	3.78
	May	20.01	9.12	11.47	2.86	8.53	4.27
	Jun	24.16	9.32	15.54	2.60	8.61	4.31
	Jul	22.99	9.46	14.50	2.92	8.49	4.24
	Aug	20.49	10.58	12.78	4.67	7.72	3.86
	Sep	17.79	12.98	11.49	8.06	6.30	3.15
	Oct	12.42	12.85	7.47	9.13	4.95	2.48
	Nov	8.53	12.03	5.12	9.47	3.41	1.70
	Dec	6.71	10.62	3.80	8.48	2.92	1.46
Tehran	Jan	7.92	10.32	4.33	7.73	3.59	1.79
	Feb	11.90	12.91	7.43	9.48	4.47	2.24
	Mar	15.33	11.85	9.06	7.19	6.27	3.14
	Apr	20.31	11.04	12.88	5.29	7.44	3.72
	May	24.45	9.73	16.44	3.28	8.01	4.01
	Jun	28.41	9.21	20.87	2.60	7.54	3.77
	Jul	25.67	9.32	17.68	2.76	7.99	4.00
	Aug	24.85	11.50	17.89	5.53	6.96	3.48
	Sep	21.02	14.51	15.09	9.44	5.93	2.96
	Oct	15.77	16.11	10.90	12.10	4.87	2.44
	Nov	10.01	13.28	6.31	10.43	3.70	1.85
	Dec	7.93	11.66	4.67	9.23	3.27	1.63

to choosing the proper azimuth angles in different periods are presented.

5.1. Solar radiation components on horizontal surface and clearness index

Table 2 presents the monthly mean daily horizontal global solar radiation and its calculated beam and diffuse components, the extraterrestrial solar radiation on a horizontal surface as well as the clearness index, for the six nominated major cities. Clearly, for all of the cities except Mashhad the maximum and minimum global solar radiation occur in June and December, respectively, and for Mashhad they happen in July and December, respectively. Isfahan and Shiraz enjoy the highest level of global and beam solar radiation and clearness index throughout the year and the lowest

values belong to Tabriz, which is placed in higher latitude. Making comparison reveals that although the global and beam solar radiations as well as clearness index are relatively lower in Karaj compared to those of other cities, in some months of autumn and winter Karaj enjoys from the highest values. Also, despite the overall higher solar radiation potential of Isfahan and Shiraz, the maximum global and beam radiation as well as clearness index in June are attained for Tehran.

5.2. Solar radiation components on vertically mounted solar surfaces

Table 3 shows the monthly mean total, beam and diffuse solar radiations received by the non-azimuth vertical surfaces ($\gamma=0^\circ$) and those reached on the horizontal surface for the nominated cities. It is observed that for all of the nominated cities in most

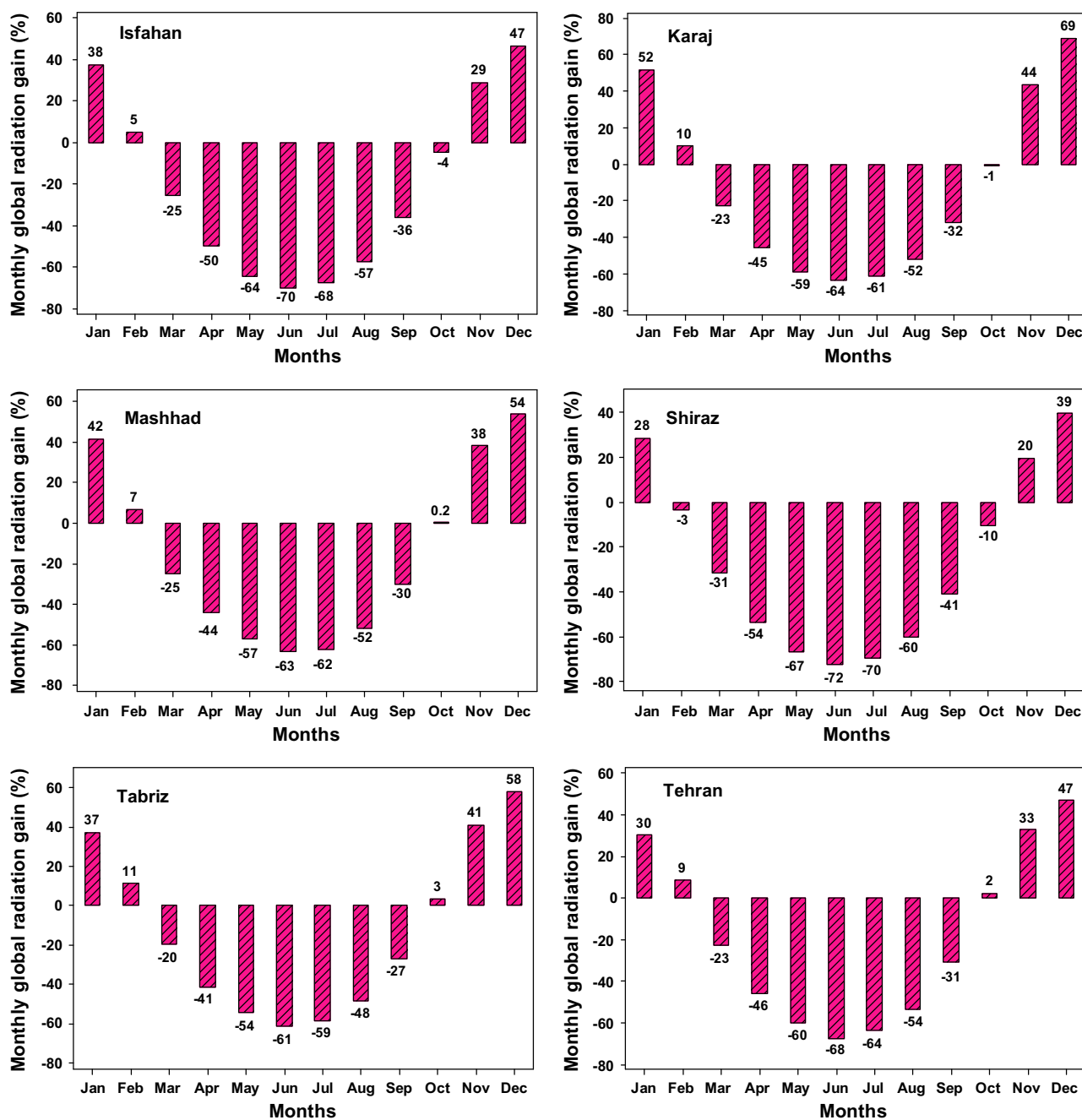


Fig. 4. The monthly global solar radiation gain (%) in the six major cities by mounting the solar surface vertically (no azimuth angle) compared to that of horizontal surface.

months of autumn and winter the total and beam solar radiation received by the non-azimuth vertical surface are higher compared to those arrived at the horizontal surface, whereas the inverse pattern is visible in spring and summer months such that they are extremely lower. In autumn and winter months the solar altitude angle is low; thus, the vertically mounted surface achieves notable increment especially for the beam component compared to that of horizontal surface. Whereas owing to higher latitude of the sun in the remaining months of the year the amount of total and beam solar radiation decline extremely. Moreover, the diffuse radiation received by the vertically mounted surface is lower in all of the months compared to that of horizontal surface. In general, with increasing the latitude the solar altitude angle decreases; thus the vertically mounted solar surfaces at lower latitudes lose more solar radiation. Therefore, the installation of vertically mounted solar surfaces would be more profitable in the locations with higher latitude.

To highlight the amount of global and beam solar radiation received by the vertically mounted surfaces at no azimuth angle compared to those of a horizontal surface, the relative global and beam solar radiation gain in all of the months of the year are depicted in Figs. 4 and 5, respectively. It should be noted that the negative gain means the loss of solar energy occurred for the vertical surface compared to that of the horizontal surface. The highest beam solar radiation gain varies between 59% for Shiraz and 124% for Tabriz. The highest global solar radiation loss varies between -72% for Shiraz and -61% for Tabriz, while the beam solar radiation loss varies from -95% for Shiraz to -83% in Tabriz.

The influence of variation in surface azimuth angle (between 0° to 90°) on the monthly mean daily total solar radiation received on the vertically mounted surfaces throughout the year, \bar{H}_V , in all of the nominated cities are shown in Fig. 6. As shown in Fig. 6, \bar{H}_V largely depends upon the surface azimuth angle and for each city

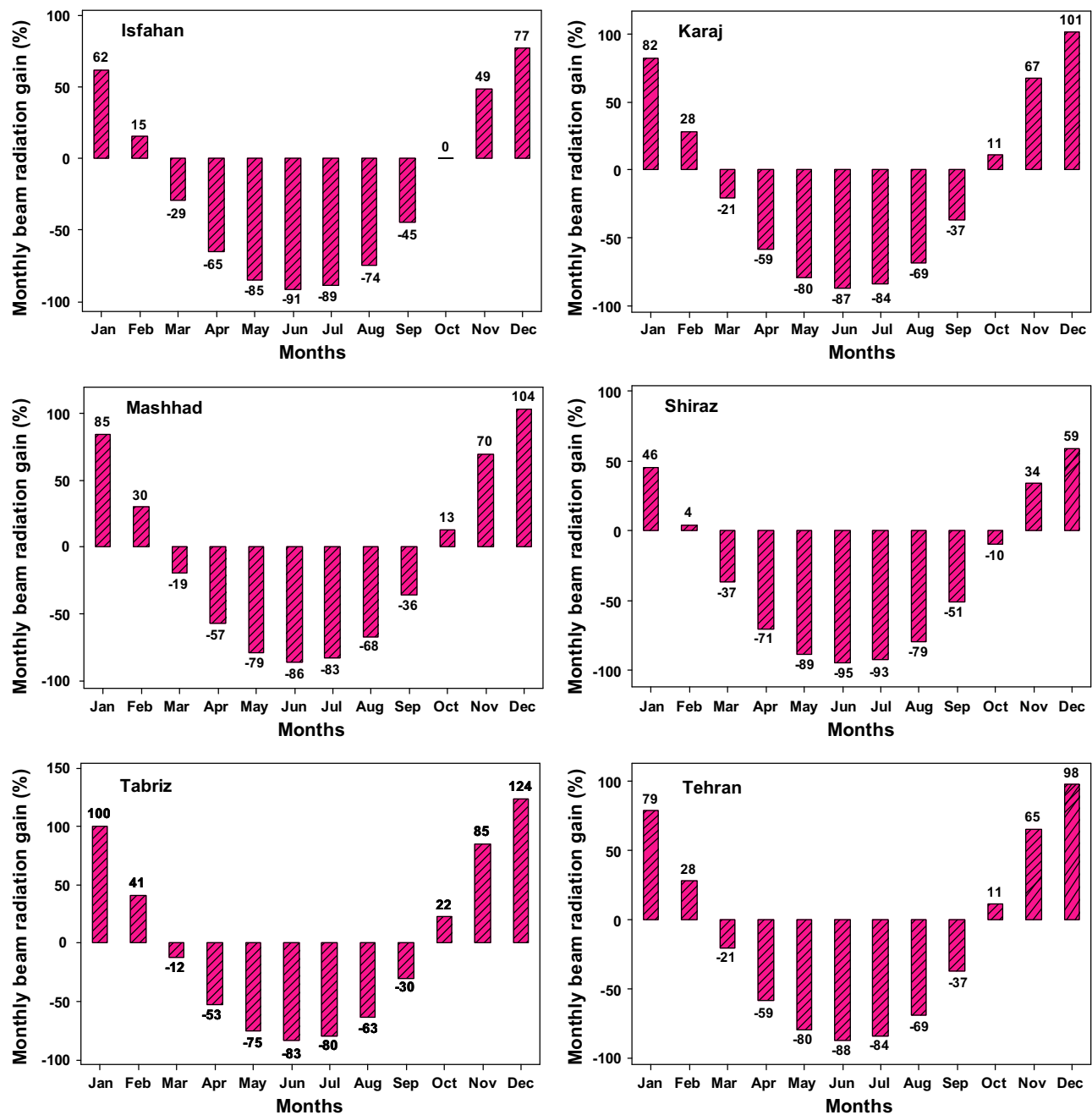


Fig. 5. The monthly beam solar radiation gain (%) in the six major cities by mounting the solar surface vertically (no azimuth angle) compared to that of horizontal surface.

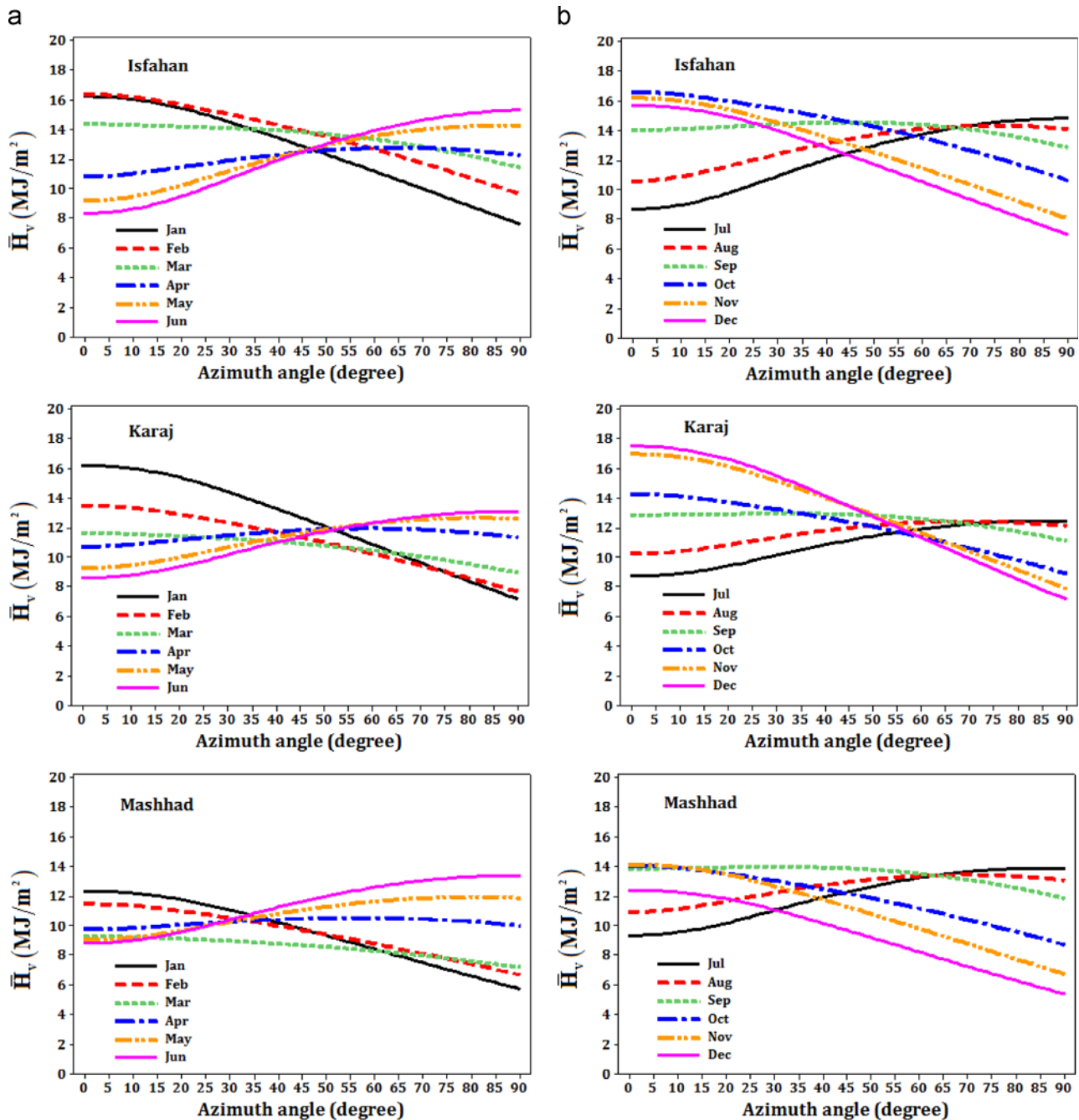


Fig. 6. Variation of monthly mean daily global solar radiation with azimuth angle for vertically mounted surfaces: (a) Jan–Jun, (b) Jul–Dec.

the variation of solar radiation with variation of azimuth angle is distinctive. As an instance, for Isfahan the monthly mean daily total solar radiation in January at azimuth angle of 0° (south direction surface) is 16.23 MJ/m^2 and is the maximum, but switching the azimuth angle to 90° (west direction surface) results in declining to 7.63 MJ/m^2 . Also, in June the monthly mean daily total solar radiation at azimuth angle of 0° is 8.32 MJ/m^2 , but with increasing the azimuth angle to 90° it reaches to the maximum value of 15.32 MJ/m^2 . The achieved results presented in Fig. 6 show that the best surface azimuth angle for vertically mounted solar surface during the six months of cold period from October to March is 0° , while in the remaining months the best angle is close to 90° .

5.3. Recognizing the better surface azimuth angles among practicable options

To identify the better azimuth angles in a particular time period, only three practical γ values of 0° , 45° and 90° , which are experienced more in Iran, have been considered. The results obtained for $\gamma=45^\circ$ and $\gamma=90^\circ$ are identical to those of -45° and -90° , respectively. Table 4 presents the monthly mean daily global and beam solar radiations on vertically mounted surfaces at the azimuth angles of 0° , 45° and 90° for all of the six nominated cities. It is observed that the maximum values of global and beam solar radiation for the period of October–March (colder period) are

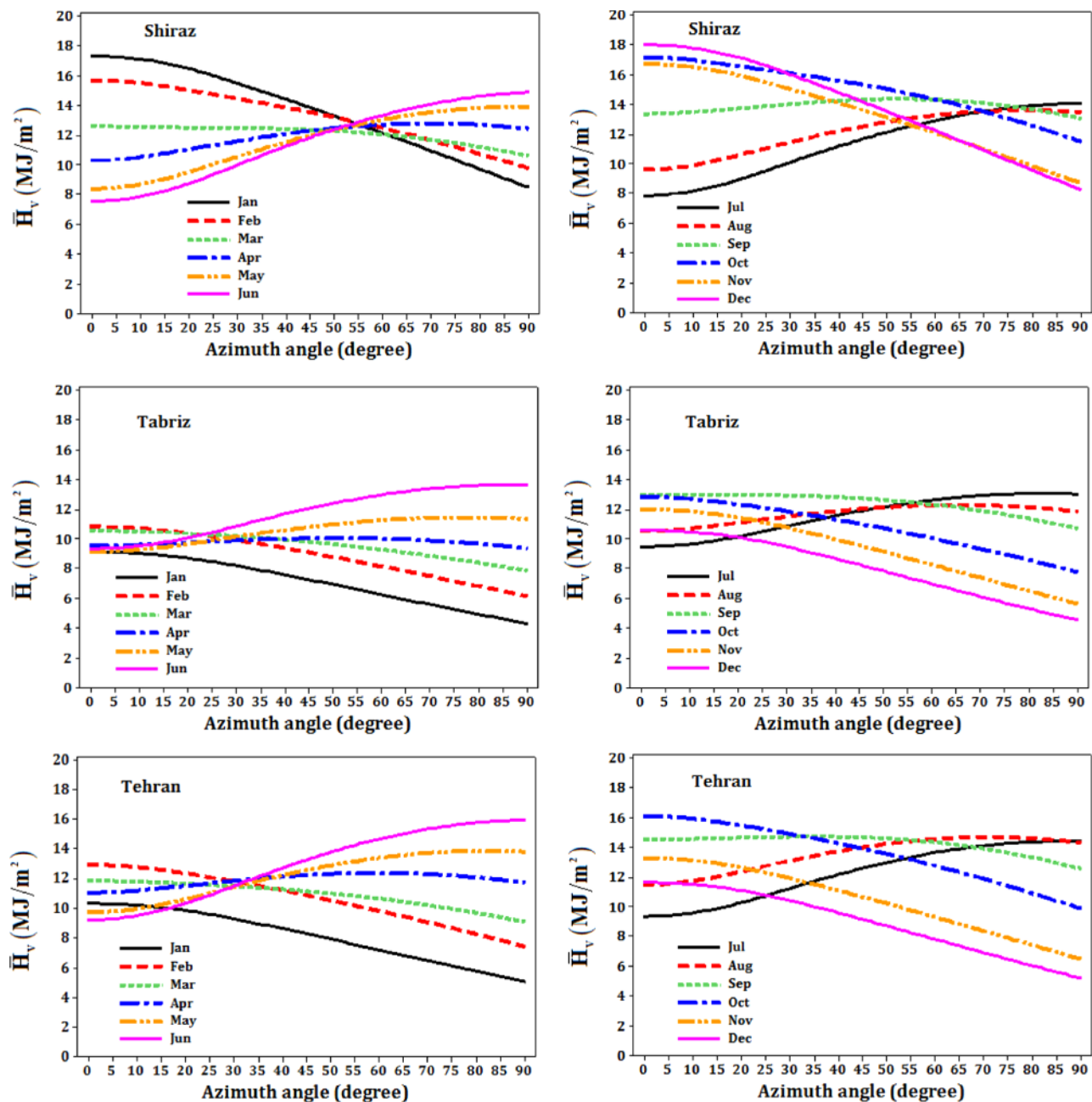


Fig. 6. (continued)

achieved at azimuth angle of 0° (i.e. south direction) for all of the cities. Therefore, it can be concluded that the south walls of buildings are the best option for installing the solar collectors and PV panels in the cold period of the year or for heating applications. The results also indicate that the highest global and beam solar radiation values for the months of April to September, or warmer period of the year, are achieved at azimuth angle of 90° (i.e. west direction) for all of the six nominated cities. Thus, the west walls of building are appropriate to mount the solar surfaces vertically in the warm period of the year to receive more solar radiation, particularly for cooling applications.

For the colder period of the year (October–March), the relative global solar radiation received by vertical surfaces at azimuth angles of 0°, 45° and 90° compared to that of horizontal surface, named case (A), case (B) and case (C), respectively, are presented in Table 5 for all of the cities. According to the results obtained for the case (A), the amount of total solar radiation gain in the six

months of the cold period of the year is positive and truly satisfactory for all of the nominated cities. Therefore, the south walls of buildings are appropriate places for mounting the solar surfaces at cold period of the year. For case (B) the solar radiation gain values are negative for all of the cities; however, the losses are not significant, thus it is placed in the second rank. It is also seen that for the case (C) compared to the horizontal surface the amount of solar radiation loss is significant; consequently, the vertical walls, with azimuth angle of 90°, are not proper places for mounting the solar surfaces at cold period of the year. To show the significance of employing case (A), the amount of relative enhancement (RE) that can be attained by employing case (A) instead of case (B) or case (C), named as RE (B→A) and RE (C→A), are presented in the last two columns of Table 5, respectively.

Table 6 shows the relative global solar radiation received by the vertically mounted surface at azimuth angle of 0°, 45° and 90°

Table 4The monthly mean daily global and beam solar radiation (MJ/m²) on vertically mounted surfaces at practicable azimuth angles of 0°, 45° and 90° in the six nominated cities.

Location	Months	$\gamma = 0^\circ$	\bar{H}_V	\bar{H}_{bV}	$\gamma = 45^\circ$	\bar{H}_V	\bar{H}_{bV}	$\gamma = 90^\circ$	\bar{H}_V	\bar{H}_{bV}
Isfahan	Jan		16.23	13.24		12.87	9.89		7.63	4.64
	Feb		16.38	12.39		13.91	9.92		9.64	5.65
	Mar		14.38	9.43		13.84	8.89		11.42	6.47
	Apr		10.84	4.97		12.47	6.60		12.27	6.40
	May		9.17	2.72		12.55	6.10		14.24	7.79
	Jun		8.32	1.72		12.48	5.88		15.32	8.72
	Jul		8.67	2.16		12.51	6.00		14.82	8.31
	Aug		10.61	4.57		13.43	7.39		14.10	8.06
	Sep		14.01	8.80		14.56	9.35		12.86	7.64
	Oct		16.60	12.36		14.57	10.33		10.63	6.39
	Nov		16.20	13.04		13.04	9.88		8.04	4.89
	Dec		15.70	12.93		12.30	9.52		7.00	4.22
Karaj	Jan		16.20	13.50		12.69	9.99		7.18	4.48
	Feb		13.51	10.07		11.35	7.92		7.71	4.27
	Mar		11.66	7.00		10.95	6.30		8.94	4.29
	Apr		10.75	5.02		11.84	6.12		11.32	5.60
	May		9.26	2.84		11.61	5.19		12.61	6.19
	Jun		8.58	1.89		11.37	4.68		13.12	6.43
	Jul		8.69	2.18		11.14	4.62		12.46	5.94
	Aug		10.22	4.22		11.99	5.99		12.12	6.12
	Sep		12.86	7.75		12.90	7.80		11.12	6.02
	Oct		14.28	10.27		12.38	8.38		8.90	4.90
	Nov		16.97	14.10		13.45	10.58		7.88	5.01
	Dec		17.50	15.03		13.47	10.99		7.16	4.68
Mashhad	Jan		12.34	9.75		9.78	7.19		5.73	3.14
	Feb		11.49	8.17		9.69	6.38		6.68	3.37
	Mar		9.26	4.90		8.66	4.30		7.18	2.82
	Apr		9.72	4.15		10.47	4.91		9.96	4.39
	May		9.02	2.67		11.06	4.70		11.87	5.52
	Jun		8.78	2.08		11.62	4.91		13.39	6.69
	Jul		9.31	2.74		12.27	5.70		13.88	7.30
	Aug		10.93	4.93		12.94	6.93		13.06	7.06
	Sep		13.84	8.77		13.87	8.81		11.84	6.78
	Oct		14.07	10.12		12.17	8.22		8.71	4.76
	Nov		14.14	11.34		11.28	8.48		6.74	3.93
	Dec		12.41	10.03		9.69	7.31		5.40	3.02
Shiraz	Jan		17.31	14.05		13.85	10.60		8.48	5.23
	Feb		15.67	11.42		13.54	9.29		9.76	5.52
	Mar		12.62	7.49		12.38	7.26		10.62	5.49
	Apr		10.29	4.33		12.30	6.34		12.44	6.48
	May		8.37	1.92		11.95	5.51		13.92	7.47
	Jun		7.54	0.98		11.83	5.26		14.90	8.33
	Jul		7.84	1.33		11.66	5.15		14.10	7.59
	Aug		9.59	3.47		12.51	6.39		13.47	7.35
	Sep		13.37	8.01		14.32	8.97		13.05	7.69
	Oct		17.16	12.74		15.31	10.89		11.49	7.07
	Nov		16.70	13.29		13.60	10.18		8.69	5.27
	Dec		18.00	14.95		14.16	11.11		8.25	5.20
Tabriz	Jan		9.12	6.84		7.27	4.99		4.33	2.05
	Feb		10.85	7.75		9.09	5.99		6.15	3.04
	Mar		10.58	6.24		9.78	5.44		7.86	3.51
	Apr		9.51	4.11		10.01	4.61		9.35	3.95
	May		9.12	2.86		10.81	4.54		11.36	5.09
	Jun		9.32	2.60		12.04	5.32		13.66	6.93
	Jul		9.46	2.92		11.86	5.32		13.04	6.50
	Aug		10.58	4.67		12.02	6.11		11.85	5.95
	Sep		12.98	8.06		12.75	7.82		10.71	5.78
	Oct		12.85	9.13		11.03	7.31		7.79	4.07
	Nov		12.03	9.47		9.57	7.02		5.67	3.11
	Dec		10.62	8.48		8.28	6.15		4.55	2.42
Tehran	Jan		10.32	7.73		8.28	5.69		5.05	2.47
	Feb		12.91	9.48		10.88	7.45		7.44	4.01
	Mar		11.85	7.19		11.15	6.48		9.09	4.42
	Apr		11.04	5.29		12.23	6.48		11.70	5.95
	May		9.73	3.28		12.56	6.10		13.79	7.34
	Jun		9.21	2.60		13.26	6.65		15.89	9.28
	Jul		9.32	2.76		12.59	6.03		14.40	7.84
	Aug		11.50	5.53		14.00	8.03		14.29	8.32
	Sep		14.51	9.44		14.67	9.60		12.56	7.49
	Oct		16.11	12.10		13.92	9.91		9.86	5.85
	Nov		13.28	10.43		10.66	7.81		6.49	3.64
	Dec		11.66	9.23		9.16	6.73		5.22	2.79

Table 5

The global solar radiation gain (%) of vertical solar surfaces at $\gamma=0, 45$ and 90° in the cold period (cases A, B and C) and relative enhancement (RE) achieved by applying case A instead of case B or C.

Location	Case A (%)	Case B (%)	Case C (%)	RE (B→A) (%)	RE (C→A) (%)
Isfahan	9.33	−7.80	−43.07	18.58	75.66
Karaj	20.77	−0.44	−46.99	21.31	88.65
Mashhad	14.90	−4.49	−45.14	20.30	82.27
Shiraz	3.58	−11.96	−41.22	17.65	70.12
Tabriz	15.49	−3.79	−44.97	20.05	81.71
Tehran	10.56	−6.99	−43.32	18.86	76.43

Table 6

The global solar radiation gain (%) of vertical solar surfaces at $\gamma=0, 45$ and 90° (cases D, E and F) in the warm period and relative enhancement (RE) achieved by applying case F instead of cases D or E.

Location	Case D (%)	Case E (%)	Case F (%)	RE (D→F) (%)	RE (E→F) (%)
Isfahan	−58.54	−47.52	−43.75	35.69	7.19
Karaj	−52.86	−44.67	−43.19	20.53	2.68
Mashhad	−52.52	−44.33	−42.96	20.13	2.45
Shiraz	−61.36	−49.45	−44.49	43.65	9.80
Tabriz	−49.88	−42.88	−42.49	14.76	0.69
Tehran	−54.87	−45.19	−42.90	26.52	4.19

compared to that of horizontal surface in the warm period of the year (April–September), named cases (D), (E) and (F), respectively. The achieved results demonstrate that as the values of solar energy gains for all of the cases are negative, mounting the solar surfaces on the vertical walls at warmer period of the year leads to loss of great amount of solar energy; nevertheless, it is found that applying the case (F) is more suitable compared to the cases (D) and (E). As a consequence, in case of utilizing solar surfaces at warm period of the year, or for cooling applications, the buildings' west walls are recommended. The amount of relative enhancement (RE) which may be obtained by applying case (F) instead of case (D) or case (E) named as RE (F→D) and RE (F→E) are presented in the last two columns of Table 6, respectively.

6. Conclusions

With adoption of horizontal solar radiation data and using the KT solar radiation model, this study aimed at estimating the amount of solar radiation components received by vertically mounted solar surfaces as well as identifying their better surface azimuth angle in six Iranian major cities of Isfahan, Karaj, Mashhad, Shiraz, Tabriz and Tehran. Owing to the similarity of the results for the surfaces with similar azimuth angle (γ) either toward west or east only positive angles in the range of $0^\circ \leq \gamma \leq 90^\circ$ were considered for the analysis. The main outcomes of this study are summarized in the following:

- I. For all cities the total and beam solar radiations arrived at non-azimuth vertical surface are higher compared to those arrived at the horizontal surface in most months of autumn and winter, while in an inverse pattern, they decrease extremely in spring and summer months compared to those of the horizontal surface. However, in all of the months the amount of diffuse radiation is less than that of horizontal surface.
- II. For non-azimuth vertical surfaces, the highest relative global and beam solar radiation gains for all cities are happen in December, owing to low solar altitude angle, whereas the highest relative solar radiation losses occur in June because of higher solar altitude. The highest global and beam solar radiation gains and losses generally increase with increasing the latitude of the location.

The total radiation received on a vertical surface, \bar{H}_V , largely depends on its azimuth angle and for each city the variation of solar radiation with variation of azimuth angle is distinctive.

- III. As to determine the better azimuth angles, five practicable angles of $0^\circ, 45^\circ, -45^\circ, 90^\circ$ and -90° were considered. Based upon the results, the maximum global and beam solar radiation in the months of October–March (the six months of cold period) attain at γ of 0° (i.e. south direction); consequently, the south walls of buildings are introduced as the best option for installing the solar collectors and PV panels in the colder period of the year or for heating applications. Also, in the hot period of the year the surfaces at γ of 90° or -90° (i.e. west or east directions) achieve the highest solar radiation values; therefore, the buildings' west walls are an appropriate place to mount the solar surfaces for cooling applications.

Acknowledgements

The authors would like to express their deep appreciation to the Energy Research Institute of the University of Kashan for supporting this study (Grant no. 1393/363447/1). The first author would love to thank his big brother Mr. Kamran Mohammadi for his continuous supports and encouragements. Also the authors acknowledge the Iranian Meteorological Organization (IMO) for the supply of raw solar radiation data.

References

- [1] Tyagi VV, Rahim NAA, Rahim NA, Selvaraj JA/L. Progress in solar PV technology: research and achievement. *Renewable Sustainable Energy Rev* 2013;20:443–61.
- [2] Sinha S, Chandel SS. Review of software tools for hybrid renewable energy systems. *Renewable Sustainable Energy Rev* 2014;32:192–205.
- [3] Tyagi VV, Panwar NL, Rahim NA, Kothari R. Review on solar air heating system with and without thermal energy storage system. *Renewable Sustainable Energy Rev* 2012;16:2289–3303.
- [4] Rustemli S, Dincer F, Unal E, Karaaslan M, Sabah C. The analysis on sun tracking and cooling systems for photovoltaic panels. *Renewable Sustainable Energy Rev* 2013;22:598–603.
- [5] Siva Reddy V, Kaushik SC, Ranjan KR, Tyagi SK. State-of-the-art of solar thermal power plants—a review. *Renewable Sustainable Energy Rev* 2013;27:258–73.
- [6] Chen GQ, Yang Q, Zhao YH, Wang ZF. Nonrenewable energy cost and greenhouse gas emissions of a 1.5 MW solar power tower plant in China. *Renewable Sustainable Energy Rev* 2011;15:1961–7.
- [7] Djurdjevic DZ. Perspectives and assessments of solar PV power engineering in the Republic of Serbia. *Renewable Sustainable Energy Rev* 2011;15:2431–46.
- [8] Renewables 2014 global status report. (www.ren21.net); 2014 [accessed June 25, 2014].
- [9] Pirasteh G, Saidur R, Rahman SMA, Rahim NA. A review on development of solar drying applications. *Renewable Sustainable Energy Rev* 2014;31:133–48.
- [10] Alamdari P, Nematollahi O, Alemrajabi AA. Solar energy potentials in Iran: a review. *Renewable Sustainable Energy Rev* 2013;21:778–88.
- [11] Thirugnanasambandam M, Iniyas S, Goic R. A review of solar thermal technologies. *Renewable Sustainable Energy Rev* 2010;14:312–22.
- [12] Khalil SA, Shaffie AM. A comparative study of total, direct and diffuse solar irradiance by using different models on horizontal and inclined surfaces for Cairo, Egypt. *Renewable Sustainable Energy Rev* 2013;27:853–63.
- [13] Psiloglou BE, Kambezidis HD. Estimation of the ground albedo for the Athens area, Greece. *J Atmos Sol Terr Phys* 2009;71:943–54.
- [14] Newland FJ. A study of solar radiation models for the coastal region of South China. *Sol Energy* 1989;43(4):227–35.
- [15] (<http://www.prweb.com>); 2014 [accessed March 20, 2014].
- [16] Bahrami M, Abbaszadeh P. An overview of renewable energies in Iran. *Renewable Sustainable Energy Rev* 2013;24:198–208.
- [17] Liu BYH, Jordan RC. Daily insolation on surfaces tilted toward the equator. *Trans ASHRAE* 1962;67:526–41.
- [18] Temps RC, Coulson KL. Solar radiation incident upon slopes of different orientations. *Sol Energy* 1977;19:179–84.
- [19] Bugler J. The determination of hourly insolation on an inclined plane using a diffuse irradiance model based on hourly measured global horizontal insolation. *Sol Energy* 1977;19:477–91.
- [20] Hay JE. Calculation of monthly mean solar radiation for horizontal and inclined surfaces. *Sol Energy* 1979;23:301–30.

- [21] Klucher TM. Evaluating model to predict insolation on tilted surfaces. *Sol Energy* 1979;23:111–4.
- [22] Steven MD, Unsworth MH. The angular distribution and interception of diffuse solar radiation below overcast skies. *Q J R Meteorol Soc* 1980;106:57–61.
- [23] Klein SA. Calculation of monthly average insolation on tilted surfaces. *Sol Energy* 1977;19:325–9.
- [24] Skarveit A, Olseth JA. Modeling sloped irradiance high latitudes. *Sol Energy* 1986;36(4):333–44.
- [25] Koronakis PS. On the choice of the angle of tilt for south facing solar collectors in the Athens basin area. *Sol Energy* 1986;36:217–25.
- [26] Willmot C. On the climatic optimization of the tilt and azimuth of flat-plate solar collectors. *Sol Energy* 1982;28:205–16.
- [27] Reindel DT, Beckman WA, Duffie JA. Evaluation of hourly tilted surface radiation models. *Sol Energy* 1990;45(1):9–17.
- [28] Perez R, Seals R, Ineichen P, Stewart R, Menicucci D. A new simplified version of the Perez diffuse irradiance model for tilted surfaces. *Sol Energy* 1987;39(3):221–31.
- [29] Perez R, Ineichen P, Seals R, Michalsky J, Stewart R. Modeling daylight availability and irradiance components from direct and global irradiance. *Sol Energy* 1990;44:271–89.
- [30] Tian YQ, Davies-Colley RJ, Gong P, Thorrold BW. Estimating solar radiation on slopes of arbitrary aspect. *Agric For Meteorol* 2001;109:67–74.
- [31] Badescu V. 3D isotropic approximation for solar diffuse irradiance on tilted surfaces. *Renewable Energy* 2002;26:221–3.
- [32] Muneer T. Solar radiation and daylight models for the energy efficient design of buildings. Architectural Press; 1997.
- [33] Klein SA, Theilacker JC. An algorithm for calculating monthly average radiation on inclined surfaces. *J Sol Energy Eng* 1981;103:29–33.
- [34] Tsalides Ph, Thanailakis A. Direct computation of the array optimum tilt angle in constant-tilt photovoltaic systems. *Sol Cells* 1985;14:83–94.
- [35] Morcos VH. Optimum tilt angle and orientation for solar collectors in Assiut, Egypt. *Renewable Energy* 1994;4(3):291–8.
- [36] Hussein HMS, Ahmad GE, El-Ghetany HH. Performance evaluation of photovoltaic modules at different tilt angles and orientations. *Energy Convers Manage* 2004;45:2441–52.
- [37] Tang R, Wu T. Optimal tilt-angles for solar collectors used in China. *Appl Energy* 2004;79:239–48.
- [38] Gunerhan H, Hepbasli A. Determination of the optimum tilt angle of solar collectors for building applications. *Build Environ* 2007;42:779–83.
- [39] Gopinathan KK, Maliehe NB, Mpholo MI. A study on the intercepted insolation as a function of slope and azimuth of the surface. *Energy* 2007;32:213–20.
- [40] Rowlands IH, Kemery BP, Beausoleil-Morrison I. Optimal solar PV tilt angle and azimuth: an Ontario (Canada) case-study. *Energy Policy* 2011;39:1397–409.
- [41] Sunderan P, Ismail AM, Singh B, Mohamed NM. Optimum tilt angle and orientation of standalone photovoltaic electricity generation. *J Appl Sci* 2011;11:1219–24.
- [42] Sun L, Lu L, Yang H. Optimum design of shading-type building-integrated photovoltaic claddings with different surface azimuth angles. *Appl Energy* 2012;90:233–40.
- [43] Talebizadeh P, Mehrabian MA, Abdolzadeh M. Prediction of the optimum slope and surface azimuth angles using the Genetic Algorithm. *Energy Build* 2011;43:2998–3005.
- [44] Jafarkazemi F, Saadabadi SA. Optimum tilt angle and orientation of solar surfaces in Abu Dhabi, UAE. *Renewable Energy* 2013;56:44–9.
- [45] Kacira M, Simsek M, Babur Y, Demirkol S. Determining optimum tilt angles and orientations of photovoltaic panels in Sanliurfa, Turkey. *Renewable Energy* 2004;29:1265–75.
- [46] Ghosh HR, Bhowmik NC, Hussain M. Determining seasonal optimum tilt angles, solar radiations on variously oriented, single and double axis tracking surfaces at Dhaka. *Renewable Energy* 2010;35:1292–7.
- [47] Lave M, Kleissl J. Optimum fixed orientations and benefits of tracking for capturing solar radiation in the continental United States. *Renewable Energy* 2011;36:1145–52.
- [48] Lubitz WD. Effect of manual tilt adjustments on incident irradiance on fixed and tracking solar panels. *Appl Energy* 2011;88:1710–9.
- [49] Maatallah T, El Alimi S, Nassrallah SB. Performance modeling and investigation of fixed, single and dual-axis tracking photovoltaic panel in Monastir city, Tunisia. *Renewable Sustainable Energy Rev* 2011;15:4053–66.
- [50] Yadav AK, Chandel SS. Tilt angle optimization to maximize incident solar radiation: a review. *Renewable Sustainable Energy Rev* 2013;23:503–13.
- [51] Mousazadeh H, Keyhani A, Javadi A, Mobli H, Abrinia K, Sharifi A. A review of principle and sun-tracking methods for maximizing solar systems output. *Renewable Sustainable Energy Rev* 2009;13:1800–18.
- [52] Khorasanizadeh H, Mohammadi K. Introducing the best model for predicting the monthly mean global solar radiation over six major cities of Iran. *Energy* 2013;51:257–66.
- [53] Khorasanizadeh H, Mohammadi K. Prediction of daily global solar radiation by day of the year in four cities located in the sunny regions of Iran. *Energy Convers Manage* 2013;76:385–92.
- [54] Duffie JA, Beckman WA. Solar engineering of thermal processes. 3rd ed.. New York, NY: John Wiley & Son; 2006.
- [55] Kalogirou SA. Solar energy engineering: processes and systems. 1st ed. Elsevier Inc; 2009.
- [56] Erbs DG, Klein SA, Duffie JA. Estimation of the diffuse radiation fraction for hourly, daily and monthly-average global radiation. *Sol Energy* 1982;28(4):293–302.